**UNIVERSIDADE FEDERAL DE MINAS GERAIS**
**Faculdade de Medicina**
**Programa de Pós-Graduação em Medicina Molecular**

Eduardo de Souza Nicolau

# INVESTIGATING THE ROLE OF PREFRONTAL NEURONS IN COGNITIVE TASKS THROUGH FIBER PHOTOMETRY AND ADAPTED BARNES MAZE PROTOCOLS

# INVESTIGANDO O PAPEL DOS NEURÔNIOS PRÉ-FRONTAIS EM FUNÇÕES COGNITIVAS, ATRAVÉS DOS PROTOCOLOS DE FOTOMETRIA DE FIBRAS E LABIRINTO DE BARNES ADAPTADO.

Belo Horizonte
2023

Eduardo de Souza Nicolau

# INVESTIGATING THE ROLE OF PREFRONTAL NEURONS IN COGNITIVE TASKS THROUGH FIBER PHOTOMETRY AND ADAPTED BARNES MAZE PROTOCOLS

# INVESTIGANDO O PAPEL DOS NEURÔNIOS PRÉ-FRONTAIS EM FUNÇÕES COGNITIVAS, ATRAVÉS DOS PROTOCOLOS DE FOTOMETRIA DE FIBRAS E LABIRINTO DE BARNES ADAPTADO.

**Versão Final**

Tese apresentada ao Programa de Pós-graduação em Medicina Molecular da Faculdade de Medicina da UFMG como requisito parcial para qualificação de doutorado.
Orientador: Professor Marco Aurélio Romano Silva (MD-PhD)
Coorientadora: Helia Tenza Ferrer (PhD)

Belo Horizonte
2023

Nicolau, Eduardo de Souza.
N639i Investigando o papel dos neurônios pré-frontais em funções cognitivas, através dos protocolos de Fotometria de Fibras e Labirinto de Barnes Adaptado [recursos eletrônicos]. / Eduardo de Souza Nicolau. - - Belo Horizonte: 2023.
33f.: il.
Formato: PDF.
Requisitos do Sistema: Adobe Digital Editions.

Orientador (a): Marco Aurélio Romano-Silva.
Coorientador (a): Hèlia Tenza Ferrer.
Área de concentração: Neurociência.
Tese (doutorado): Universidade Federal de Minas Gerais, Faculdade de Medicina.

1. Cognição. 2. Memória. 3. Fotometria. 4. Córtex Pré-Frontal. 5. Dissertação Acadêmica. I. Orientador Sobrenome, Nome. II. Coorientador Sobrenome, Nome. III. Universidade Federal de Minas Gerais, Faculdade de Medicina. IV. Título.

NLM: WL 102.5

Bibliotecário responsável: Fabian Rodrigo dos Santos CRB-6/2697

UNIVERSIDADE FEDERAL DE MINAS GERAIS
FACULDADE DE MEDICINA
PROGRAMA DE PÓS-GRADUAÇÃO EM MEDICINA MOLECULAR

**FOLHA DE APROVAÇÃO**

**INVESTIGANDO O PAPEL DOS NEURÔNIOS PRÉ-FRONTAIS EM FUNÇÕES COGNITIVAS, ATRAVÉS DOS PROTOCOLOS DE FOTOMETRIA DE FIBRAS E LABIRINTO DE BARNES ADAPTADO**

**EDUARDO DE SOUZA NICOLAU**

Tese de Doutorado defendida e aprovada, no dia trinta de dezembro de dois mil vinte e dois, pela Banca Examinadora designada pelo Colegiado do Programa de Pós-Graduação Medicina Molecular da Universidade Federal de Minas Gerais constituída pelos seguintes professores doutores:

**Marco Aurelio Romano Silva** - Orientador
UFMG

**Helia Tenza Ferrer** - Coorientadora
UFMG

**Angela Maria Ribeiro**
UFMG

**Alexandre Guimarães de Almeida Barros**
UFMG

**Bruno Silva Costa**
SCMBH

**Célio José de Castro Júnior**
IEP-SCBH

Belo Horizonte, 30 de dezembro de 2022.

Documento assinado eletronicamente por **Bruno Silva Costa**, **Usuário Externo**, em 05/01/2023, às 12:21, conforme horário oficial de Brasília, com fundamento no art. 5º do Decreto nº 10.543, de 13 de novembro de 2020.

Documento assinado eletronicamente por **Célio José de Castro Junior**, **Usuário Externo**, em 05/01/2023, às 16:11, conforme horário oficial de Brasília, com fundamento no art. 5º do Decreto nº 10.543, de 13 de novembro de 2020.

Documento assinado eletronicamente por **Alexandre Guimarães de Almeida Barros**, **Professor do Magistério Superior**, em 06/01/2023, às 10:07, conforme horário oficial de Brasília, com fundamento no art. 5º do Decreto nº 10.543, de 13 de novembro de 2020.

Documento assinado eletronicamente por **Helia Tenza Ferrer**, **Usuário Externo**, em 06/01/2023, às 20:13, conforme horário oficial de Brasília, com fundamento no art. 5º do Decreto nº 10.543, de 13 de novembro de 2020.

Documento assinado eletronicamente por **Angela Maria Ribeiro**, **Professora do Magistério Superior**, em 08/01/2023, às 17:11, conforme horário oficial de Brasília, com fundamento no art. 5º do Decreto nº 10.543, de 13 de novembro de 2020.

Documento assinado eletronicamente por **Marco Aurelio Romano Silva**, **Professor do Magistério Superior**, em 03/02/2023, às 08:32, conforme horário oficial de Brasília, com fundamento no art. 5º do Decreto nº 10.543, de 13 de novembro de 2020.

A autenticidade deste documento pode ser conferida no site https://sei.ufmg.br/sei/controlador_externo.php?acao=documento_conferir&id_orgao_acesso_externo=0, informando o código verificador **1995024** e o código CRC **9596333E**.

# RESUMO

O córtex pré-frontal medial (mPFC) é essencial na execução de tarefas cognitivas, no entanto, pouco se sabe sobre como esses neurônios são modulados durante tarefas específicas e qual subtipo de neurônios é responsável por isso. Portanto, com a intenção de abordar essa questão, registramos os padrões de ativação de neurônios gabaérgicos e glutamatérgicos do mPFC por meio de fotometria de fibra (FIP) em camundongos, enquanto realizávamos simultaneamente a tarefa cognitiva do Labirinto de Barnes (BM) (ensaio comportamental de 4 dias). Além disso, um protocolo estrutural e procedimental alterado para o BM foi validado neste estudo devido a modificações necessárias que permitiram a realização simultânea de FIP e BM. Uma validação bem-sucedida do protocolo foi seguida pelos nossos resultados preliminares, que mostraram que tanto os neurônios glutamatérgicos quanto os gabaérgicos apresentaram mudanças significativas na intensidade de ativação e no número de eventos em contextos específicos ao longo dos dias da tarefa. Além disso, quando estratificados e cruzados com parâmetros de desempenho do BM, como latência para completar as tarefas e estratégia adotada, os neurônios glutamatérgicos e gabaérgicos apresentaram uma diminuição significativa nos padrões de ativação e no número de eventos de ativação ao longo dos dias. Esses dados sugerem não apenas um papel importante dos neurônios glutamatérgicos e gabaérgicos do mPFC na aprendizagem, memória e tomada de decisões, mas também que os padrões de ativação de cada um desses grupos podem servir como marcadores de progressão e/ou disfunção cognitiva. PALAVRAS-CHAVE: Memória, Aprendizagem, Tomada de Decisões, Córtex Pré-Frontal Medial (mPFC), Fotometria de Fibra (FIP), Labirinto de Barnes (BM), Glutamatérgico, Gabaérgico, Atividade Neuronal, Padrões de Ativação Neuronal, Dinâmica Neuronal.

.

# ABSTRACT

The medial prefrontal cortex (mPFC) is essential in the execution of cognitive tasks, however very little is known on how these neurons are modulated during specific tasks and which subtype of neurons are responsible for so. Therego, with the intention of addressing this issue, we recorded mPFC gabaergic and glutamatergic activation patterns through fiber photometry (FIP) in mice, while simultaneously performing the Barnes Maze (BM) cognitive task (4 day behavioral trial). In addition, an altered structural and procedural protocol for BM was validated in this study due to necessary modifications allowing FIP and BM to happen simultaneously. A successful protocol validation was followed by our preliminary results, which showed that both glutamatergic and gabaergic neurons presented significant change in activation intensity and number of events in specific contexts throughout the task days. In addition, when stratified and crossed with BM performance parameters, such as latency to complete tasks and adopted strategy, glutamatergic and gabaergic neurons presented a significant decline in both activation patterns and number of activation events throughout the days. This data suggest not only an important role of glutamatergic and gabaergic mPFC neurons in learning, memory and decision making, but also that activation patterns of each of these groups may serve as markers for cognitive progression and/or dysfunction.
KEY-WORDS: Memory, Learning, Decision Making, Medial Prefrontal Cortex (mPFC), Fiber Photometry (FIP), Barnes Maze (BM), Glutamatergic, Gabaergic, Neuronal Activity, Neuronal Activation Patterns, Neuronal Dynamics.

# LIST OF FIGURES

# LIST OF ACRONYMS AND INITIALS

(cm) - Centimeters

(cm/s) - Centimeters per Second

(D) - Days

(m) - Meters

(mg) - Milligrams

(mL) - Milliliters

(mm) - Millimeters

(mV) - Milivolts

(n) - Numbers

(nL) - Nanoliters

(nm) - Nanometers

(s) - Seconds

A.P. - Anterior and Posterior

Avg. - Average

BM - Barnes Maze

CNS - Central Nervous System

D.V. - Dorsal and Ventral

dF/F - Variation of fluorescence of fluorescence

FIP - Fiber Photometry

GABA - Gamma-Aminobutyric Acid

Gad2 - Glutamate Decarboxylase 2

M.L. - Medial and lateral

mPFC - Medial Prefrontal Cortex

VGlut1 - Vesicular Glutamate Transporter 1

# INDEX



.

# 1. INTRODUCTION

Cognitive function is the underlying mechanism through which we constantly acquire and process information (MCDOUGALL G. J., 2019). Essentially, there are several functions that compose cognition, such as: memory, language, executive functions, and visual and spatial abilities (NOZAWA T., 2015). More precisely, through all mechanisms, including their biological understanding, in which sensory input is retained, transformed and acted upon (MCDOUGALL G. J., 2019).

To better understand cognitive functions and its cruciality, comprehending the traits of a simple face-to-face conversation over dinner will suffice. During a conversation, listening (sound) and gesture or object visualization (sight) are our main sensory inputs. A group of complex structures within our ears are capable of transforming vibrations in the air (sound waves) into cellular electrical signals (SOHMER H., 2000) , while photons (light) are perceived by cells within the retina and then electrically propagated (MANIVANNAN M., 2012), allowing us to both hear and see, respectively. Within this situation, a sensory input: an external signal transformed into cellular electrical current, will be carried out through nerves into the central nervous system (CNS), such information will propagate through a network of neurons, then be processed within this network, and allow us to evoke or store information. Overmore, a perfume (smell), a hug (touch) or even a drink (taste) add to the sensory input and to how we perceive and act upon the context of the conversation. Together, our 5 senses stimulate the nervous system from the moment we are born (some even before) giving us the perception of existence. Every single experience will serve as a sensory input, and through time define your personality and how you respond to certain stimuli (behavior) (KOOP L.K., 2021).

With the understanding of cognition in mind, cognition may be broken down into: gathering information of various stimuli (learning), storing information (memory) and assessing and acting over context and resolution (decision making) (HOLTER S.M., 2015). Moreover, cognitive function is a common and essential trait of normal behavior, and as read above, an extremely important neurological tool for day-to-day life interactions. Concerns surge when these functions are constantly disrupted, such as seen in psychiatric disorders (depression, anxiety, schizophrenia, etc…). Diseases that have significantly increased in the past decade (W.H.O). Although the existence of such disorders are known for over centuries,

dating back to 1100 B.C, for some of these diseases, science has yet to identify cause, treatment or cure (SURIS A. 2016). On the other hand, our understanding in neuroscience has also been exponential in the past few years. New techniques have been developed and allowed us to study neurology in matters that have never been imagined before. The use of high resolution imagining, electrical and chemical quantification, molecular studies, behavioral analysis, neuronal control, machine learning and a lot more have been paving the way for breakthroughs in neuroscience (GUNAYDIN., 2014).

Overall, great effort has been put in mapping the brain circuitry, not only anatomically, but also a translation into behavioral functioning. Unfortunately, as explained by Friedemann Pulvermüller, in his 2021 article, although studies have been able to associate specific networks and firing patterns to cognitive behavior, we are scratching the surface. Understanding the structural and functional traits of cognition is way more complex, since cognition itself is the junction of several neurological tasks taking place in multiple regions and traveling through collective networks formed by billions of neurons (CYBERN B., 2014).

The medial prefrontal cortex (mPFC) plays an important role in regulating cognition, emotion and behavior. mPFC neurons are extremely active throughout diverse behavior contexts, which in manners suggest that mPFC neurons are key for encoding specific behaviors (Qi X.L., 2011). Multiple clinical and preclinical studies have shown ties of the mPFC to actual outcomes (RES B.B., 2012, LEE I., 2013). However, little has been investigated regarding how specific neuronal subunits within the mPFC and their residing neuronal population act upon cognitive behavior.

The Barnes Maze protocol is considered one of the most complex behavioral apparatus for investigating cognition in mice, possessing a wide output of data ranging from learning, memory and decision making (PITTS M.W., 2018). Hence, paired with fiber photometry, a more recent technique that allows the recording of neuronal activation (GUNAYDIN., 2014) with spatial resolution and neuron specificity in freely moving mice, we believe that a more comprehensive investigation of the mPFC role in cognition may be provided.

Therefore, in this study, we aimed to investigate the activation patterns of both glutamatergic and gabaergic neurons in the mPFC through fiber photometry of mice while undergoing the Barnes Maze cognitive task.

The complete structure for this study (hardware, constructs, viruses, mice and protocols) were all developed during and specifically for the execution of these results. To sought out

investigating possible activation patterns of the mPFC glutamatergic and gabaergic neurons during the Barnes Maze task in mice, we focused on implementing the fiber photometry technique together with an adapted Barnes Maze protocol in a manner that would allow freely moving mice to fully explore the Barnes Maze apparatus while being attached to the FIP system.

# 2. METHODS

## 2.1 Ethics Statement

All procedures were approved by the animal ethics committee from the Federal University of Minas Gerais (protocol number: 288/2019 - expiration date: 03/11/2024), under the entitled project “The role of prefrontal neurons in cognitive function”.

## 2.2 Housing

Individually-housed male adult (8-12 weeks) Gad2-Cre (Jackson Laboratory Gad2tm2(cre)Zjh (010802)) and VGlut1-Cre (Jackson Laboratory Slc17a7tm1.1(cre)Hze (023527)) C57BL/6 mice were used in this experiment. Animals received proper care before, during and after experimental procedures with food and water ad libitum.

## 2.3 Barnes Maze behavioral protocol

To accurately study activation patterns of neurons during behavioral context some alterations to protocol and structure were needed for running optical cables and head stubs. The Barnes Maze apparatus is a circular platform (90 x 90 x 90 cm) with 19 false escape holes and one true escape chamber **(Fig. 03-A-G)**. Mice are allowed to explore the circular apparatus for 3 minutes, in which if the mouse is able to find the escape hole among 19 false other holes the test would end, otherwise, at the end of the test mice are forced into the true escape chamber and restricted there for 1 minute. Hence, the objective of this task is for animals to locate and enter the escape chamber accurately, and from day-to-day make less mistakes with lower latency times and distances traveled, enforcing memory,learning and decision making.

All animals were conditioned to the behavior room for 5 days before experimentation. Room light and temperature were controlled and maintained throughout the whole experiment. Two protocols were applied in this study. Protocol 1: Modified and applied for *VGlut1-Cre* and *Gad2-Cre* mice for BM+FIP paring. Protocol 2: Traditional protocol (PITTS, 2018) for WT mice as a control protocol. BM task (Stoelting Corp®.) was executed in 2 steps (habituation and training) in a total of 5 days. In step one, habituation, animals were conditioned to the apparatus allowing them one at a time, to freely explore its surface over one day for 3 minutes, of which after they were put back into their cages. For the next 4 days,

animals were subjected to BM at a rate of 3 trials/day, each trial lasting the maximum of 3 minutes, with intervals of 2 minutes in between for the altered protocols and 15 minutes of interval for the traditional protocols. Animals that managed to locate and enter the escape chamber within 3 minutes, were then restricted in the escape chamber for 1 minute and relocated to their cages, while if not, they were forced into the escape chamber and restricted for 1 minute. Structural modifications were also performed and will be shown and discussed here. Video imagining was recorded during habituation and training and each trial was recorded and analyzed in realtime using the AnyMaze software (Stoelting Corp®.). Parameters acquired during the task were: number of errors (number of wrongfully investigated holes), latency (period of time to finalize the task), distance traveled (distance traveled until the task was completed) as well as average speed during the task. These values were also stratified into primary (collected data from the moment the task started until the mouse has located the escape chamber) and total (collected data from the moment the task started until the mouse has entered the escape chamber). Search strategies were also assessed (strategy used for each animal to complete the task). A total of three strategies were considered: random (mice randomly investigate the apparatus to find the escape chamber), serial (mice locate a hole, and investigate the remaining in sequence to find the escape chamber) and direct (mice use spatial navigation to orient themselves towards the true escape chamber) .

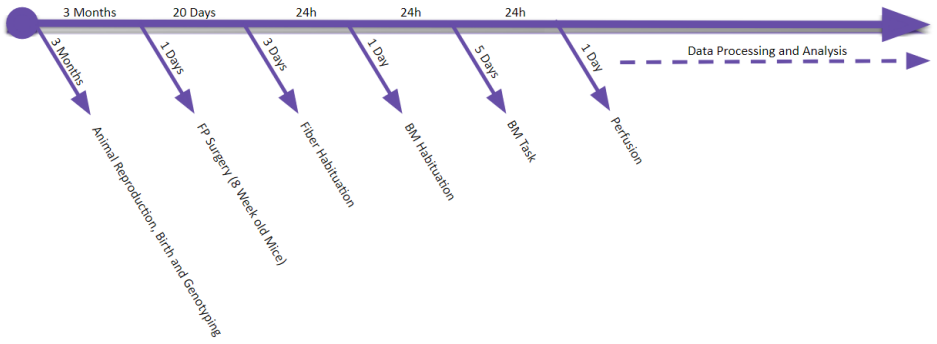


**Fig: 01 - Experimental Timeline.** Experimental timeline, from day one of animal reproduction to the final day of tissue collection and data analysis. A total of 3 months and 11 days were spent from start to data acquisition and addition 2 weeks for data processing (after data processing and statistical analysis were script written in python - 8-12 months).

In terms of experimental timeline, the protocol above does not differ from traditional protocols (PITTS., 2018). Nevertheless, due to optimization reasons, such as: constantly removing optical fibers from the animal's head and facilitating the animal's locomotion while attached to the FIP systems, structural and protocol modifications had to be made.

**2.4 Fiber Photometry**

FIP is a recently developed technique that allows the quantification of molecules and elements within specific cellular types and subtypes. Initially, it was used to exclusively quantify calcium (Ca+) surges in neurons, which due to its importance in synaptic transmission could be interpreted as neuronal activity. As of today, the technique has been adapted allowing further quantification of other substances such as neurotransmitters, other ions and even toxins. For quantifying Ca+ surges a GCaMP biosensor was developed back in 2014. This molecule is formed of a myosin 13 protein, a calmodulin (CaM), and a green fluorescent protein (GFP) in the center of both. When no calcium is present both C and N terminals of the GFP protein are sequestrated resulting in weak to undetectable fluorescence surges due to its inexcitability. However, in the presence of Ca+ ions, both terminals are brought in together again, resulting in an excitable GFP. Hence, by focusing light in a responsive spectrum over the biosensor when binded to Ca+ the equipment is able to detect fluorescent emissions and convert such signals to electrical and digital data. Signals have to make way from cells within mice to the converting equipment, and vise-versa. To do so, while subjected to FIP, animal models must express the biosensor through transgenic modification or viral injections and through transcranial optical fiber implants attached to the models and the equipment, transmit the signals.

In this study, we used a transgenic Cre restriction approach. Two groups of mice presented expressions of a cre-recobniase protein attached downstream to VGlut1 or Gad2 genes, which in term are exclusively expressed in glutamatergic and gabaergic neurons, respectively. By injecting a biosensor cre-dependent DNA sequence through viral vectors we were able to restrict the biosensor expression to targeted types of neurons.

In this study, light was generated at 405 isosbestic, 10 µW - 88 mA, and 465, 30 µW - 393 mA, nm (for the 2x2 Doric Studio system rig) at tip and used to excite the jGCaMP6f biosensor. For optimal light generated, an optical power meter (THORLABS®: PM100D) was used. FIP signals were collected at a sampling frequency of 12 kBs/s in an interleaved manner (10 ms windows - between 405 and 465) for 535 nm and then amplified using Doric's direct current 10x scale amplifier. Before each day of experimentation all patch cords were light saturated at the same intensities above for 1 hour to avoid absorbance during the experiment. 405 nm signals were used to collect excitation/emission of jGCaMP6f fluorescence at its isosbestic point which was used to determine background (non–calcium-dependent) fluorescence levels. The FIP rig system was acquired from Doric

Studio and data was collected in the Doric Studio software. To overlap behavioral parameters and FIP data, we connected both Doric Studio and AnyMaze through the AMI-2 interface hardware (Stoelting Corp®.).

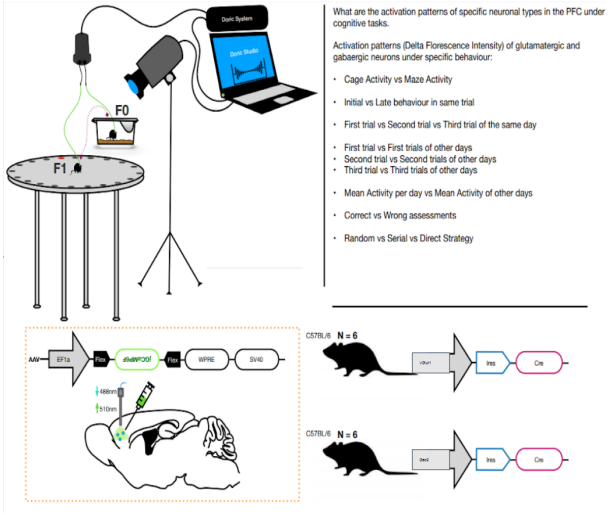


**Fig: 02 - Experimental layout.**

Fiber photometry layout over Barnes Maze learning, memory and decision making apparatus, performed in both Gad2-Cre and VGlut1-Cre positive mice. Both transgenic mice carrying the Cre recombinase enzyme under the mult-ribosomal structures internal ribosome entry site (IRES) were injected with an adeno associated virus (SV40) over the medial prefrontal cortex (M.L. ≤ +0.35 mm, A.P. ≤ +2.4 mm, +D.V. ≤ 1.8 mm) carrying the EF1a essential cell promoter, flanked jGCaMP6f (Cre-dependent - calmodulin green fluorescent indicator) biosensor and Woodchuck Hepatitis Virus Posttranscriptional Regulatory Element (WPRE) expression enhancer and SV40.

## 2.5 Viral injection and optic fiber implantation - surgical procedures

Animals were anesthetized with Xylazin (ANASEDAN® 2%) at 80 mg/kg and Ketamine (DOPALEN® 10%) at 8 mg/kg given intraperitoneally. After 10 minutes, animals were put in an anesthesia chamber and vaporizer from (VetEquip®: 901305 and 931503) and further sedated with 2% isoflurane carried by oxigen at a volume of 1 L/min for 5 minutes. Toe pinch technique was used to test animal reflexes. In sequence, the surgical site (scalp) was shaved down with an electric blade (Philips® Multigroom: QG3340/16) and then placed over a stereotaxic (KOPF®: 940) heating pad (KOPF®: TCAT-2LV) with an isoflurane anesthesia mask (KOPF®: 923-B). Ophthalmic ointment (ALCON®: TobraDex - Dexamethasone 1 mg/g: 631) was applied to the eyes to prevent drying. A midline incision was made with surgical scissors down the scalp and, in sequence, using a dental drill (WPI®: R114JQ049) we performed a craniotomy in the mPFC at 0.35 mm (M.L.) and 2.4 mm (A.P.) from bregma. Stereotaxic coordinates were confirmed in the digital interface sistem from KOPF®. Viral delivery of AAV-jGCaMP6f-FLEX-WPRE-SV40 (Deisseiroth lab - material transfer agreement (MTA) documented) at 500 nL (≥ $4\times10^{12}$ vg/mL) was injected at (M.L.), 2.4 mm (A.P.) and 1.8 mm (D.V.) through a glass needle controlled by a digital nano-injector (WPI® Micro4: 161120-12E). 2.2 mm mono optic fiber canulas (Doric studio: MFC_100/125-0.66_2.2mm_ZF1.25(g)_FLT) were implanted at the exact coordinates of viral transfection. To hold the implants in place, surgical cement (Parkell® METABOND C & B: S380) was applied around the site avoiding skin and eye contact. Surgical glue (3M® VetBond: 1469SB) was used to suture the skin around the implant. 50 µL of Ketoprofen

(PROFENID® 100 mg: 20ML) at 5mg/kg were diffused in 500 µL of ringer's lactate solution (SANOBIOL LAB®: 7898153652145) and administered subcutaneously for 3 days as post-surgical care. Additionally, 2% lidocaine XYLESTESIN 5% (Cristal Pharma®) was infiltrated using a drop bottle in the incision site and underlying tissues. Animal's were weighted pre and post-surgical for 5 days after surgical procedures and 1 day before experimentation. A total of 20 days were waited before experimentation for optimal viral transfection. Any animal with weight loss higher than 10% of its initial weight was removed from the experiment .

### 2.6 Statistics and Data Processing

For behavior experiments all data were analyzed as either parametric (paired or unpaired) one way or two way anova and post hoc Tuket's test for multiple comparisons when significant. Data and formulas were processed in the Anymaze behavior software and analyzed in GraphPad Prism. For FIP analyses, a Z-Score approach was chosen. The mPFC is a region of large activity with higher baseline measurements due to its purpose, hence, traditional methods would hide significant differences, if any. Z-Score itself represents how far a data point is from the average population by plotting the impact of point deviation from baseline within a scale from -3 to +3. Data presented with 2 or more scale deviations are considered significant. All data plots explore variations within Z-Score intensity, hence when statistically analyzing either number of events or the intensity of these events only values above two were considered.

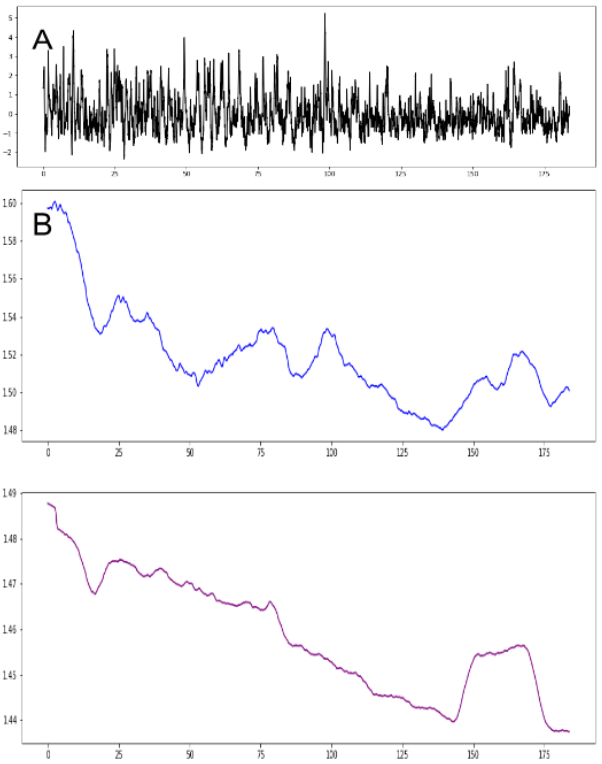


FIP data and analysis was executed in multiple steps. Data was first processed in Google's Colab python based software. To do so, we based our scripting in Ekaterina Martianova 2019 FIP data analysis with her assistance (request author for access). New functions and adaptations were inserted into the script to better fit both our FIP parameters

and the Barnes Maze behavior. NeuronalInitially, since acquisition was done at 12000 points per second and the mPFC is a highly responsive area, the presented data was very clustered **(Fig. 3-A)** (Clustered data - y axis (millivolts - mV) and x axis (time - seconds)). Hence, we smoothed the signal acquisition for both 405 - purple and 465 - blue data while also rescaling the data graph to better visualize signal dynamics **(Fig. 3-B)**(Smoothing - y axis (millivolts - mV) and x axis (time - seconds)). Smoothing allowed us to remove proximal data points within a range of 100 data points, unifying them into one, giving the data a more suave appearance. Baseline parameters were then determined by tracing a line within each data plot signal to eliminate any fissure (electrical oscillations, photobleaching, patch saturations and motion interference) that could interfere in the analysis **(Fig. 3-C)**(Baseline marking - y axis (millivolts - mV) and x axis (time - seconds)). The baseline model assumed best fit for the background signal 405, while allowing 465 to simply follow the determined curvature. In conjunction to the the baseline removal, over 2000 initial and end points were removed from each data set to eliminate light bleaching (natural occurring decline in photon emission capability) and oscillations due to on and ff electrical input to the system **(Fig. 3-D)**(Interference removal - y axis (millivolts - mV) and x axis (time - seconds)). Next both signals were graph-rescaled **(Fig. 3-E)** (Rescaling - y axis (millivolts - mV) and x axis (time - seconds)) to allow overlap visualization of both 535 signals provenient from 405 and 465 excitation. **(Fig. 3-F)**(Isobestic and GCaMP overlapping - y axis (millivolts - mV) and x axis (time - seconds)). In sequence, 535 signal data from

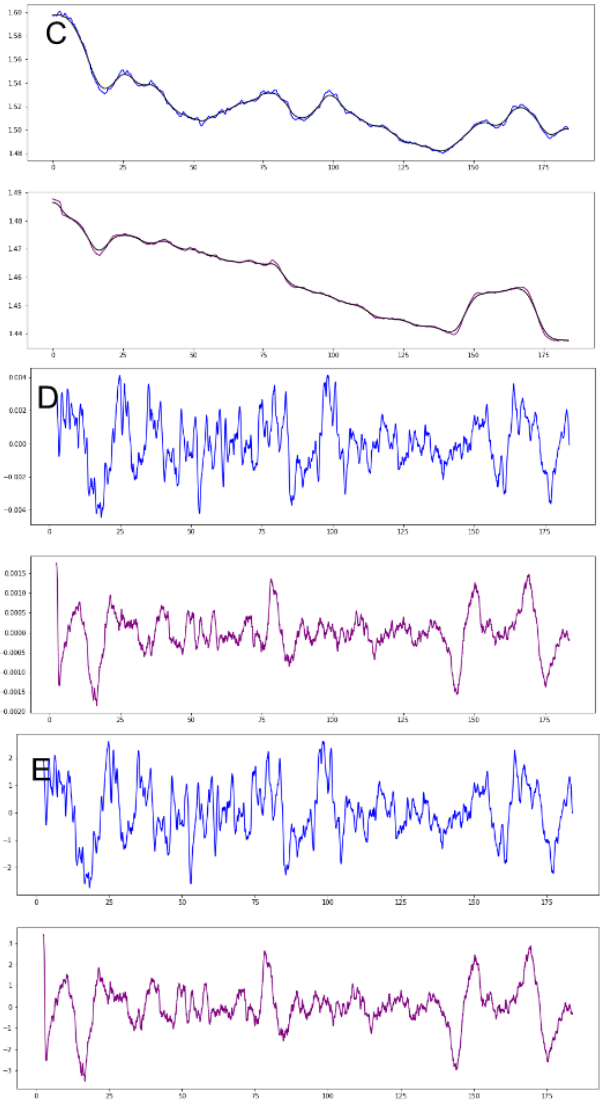


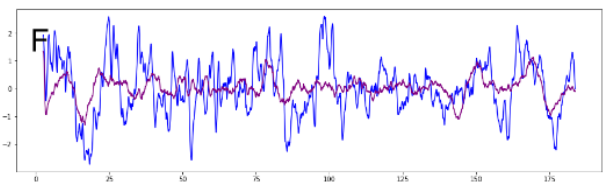

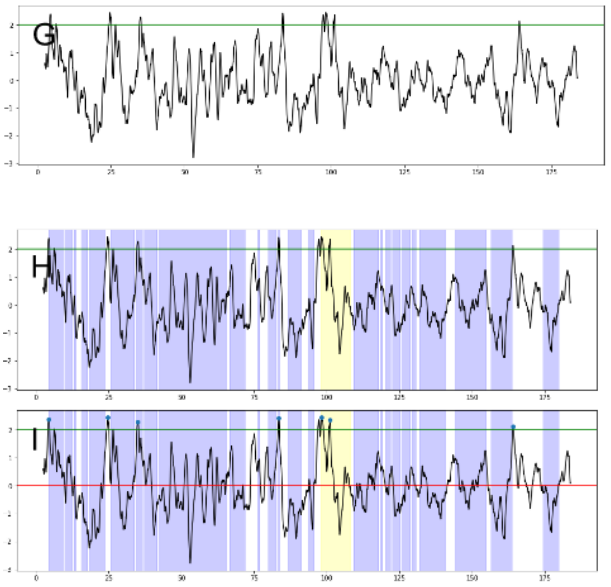


465 excitation was fit to 535 isosbestic data provenient from 405 excitation **(Fig. 3-G)** through the dF/F (F - median(F)) / median(F) function and analyzed through the Z-Score formula z (x –) / σ, where x = spiking signals, μ = mean data signal and σ = standard deviation.Together an additional data set was added to the analysis shading behavioral periods over time and neuronal cinetics (blue shading: error holes investigated - yellow shading: escape chamber investigation) **(Fig. 3-H)**. All data with a significant z-score of 2 or more deviations from the baseline were extracted, separated into 4 groups (Chamber peak activity, error hole peak activity, non-paired peak activity and total peak activity) and analyzed in the Prism GraphPad software **(Fig. 3-I)**. Data for the number of occurring peaks were also calculated.

**Fig: 03 - Analysis guide for FIP**
A-Raw data with no processing, B-Data Smoothing, C-Baseline Marking, D-Interference Removal, E-Rescaling
F-Isosbestic and GCaMP Overlapping, G-Data Fitting, H-Behavioral Input, I-Peak Detection

# 3. RESULTS

To adapt the BM structure and protocol allowing FIP, we fabricated a metal structure with an adjustable shelf height. **(Fig. 4-H).** This structure allowed us to place the equipment 2 meters above ground (1 meter and 10 centimeters above BM) solving wiring and patch cord obstacles while keeping commutators viable. Moreover, we 3D printed a small wall blockade **(Fig. 4-H)** to prevent mice from going too deep into the escape chamber and damaging the implant and patch cords placed over their heads. As for restricting mice in the escape chamber **(Fig. 4-D-H)** after they have entered it **(Fig. 4-A)**, using the traditional lid **(Fig. 4-C)** was not possible due to the cords attached to the mouse's head, in this case a second piece was 3D printed to block but still allow wiring passage **(Fig. 4-B)**. Both 3D printed projects have been made available at thingverse, free of cost. Therefore, adaptable for any mouse based cognitive behavior, the layout used here allows both fiber photometry in two distinct areas, with two or more wavelengths per area, height adjustable commutator for different apparatus sizes and doric studio (fiber photometry data acquisition) - AnyMaze (mouse behavior data acquisition) interface linkage, allowing synchrony in fiber activity and mouse behavior **(Fig. 04-F-G-H)**. In addition, data processing and analysis for FIP and behavior data overlap were specifically scripted in Google's Colab python based online software. A total of 14 mice, 6 Gad2-Cre C57BL6 and 6 VGlut1-Cre C57BL6 **(Fig. 02)** underwent surgical (mPFC AAV-ELFa-jGCaMP6f viral injection and fiber optic implantation), behavioral and FIP procedures, of which 2 Gad2-Cre and 1 VGlut1-Cre were excluded due to not finish the procedures in consequence of one of the following reasons: low viral transfection, broken or loose optic fiber or succumbing to during surgical procedures. All of the remaining mice filled inclusion criteria.

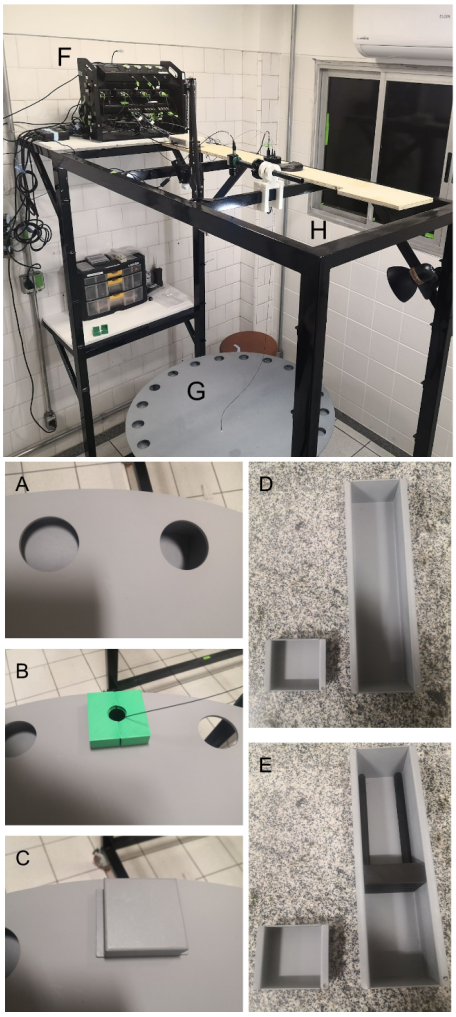

**Fig: 04 - Barnes maze adaptations for simultaneous fiber photometry.**

**A:** Left: false escape hole and Right: escape chamber. Both attached to the BM structure
**B:** Adapted 3D printed lid for escape chamber.
**C:** Old lid for escape chamber.
**D:** Left: false escape hole and Right: escape chamber. Both detached from the BM structure.
**E:** Left**:** false escape hole and Right: escape chamber with wall blockade.
**F:** Fiber photometry structure from doric studios in-lab assembled.
**G:** Barnes Maze apparatus.
**H:** Adaptable metallic structure for FIP and behavioral studies.

### 3.1 Although distinct, BM adapted structure and protocol present similar cognitive performance rates to traditional layouts.

We initiate our study by analyzing the performance of 20 (6 Gad2-Cre, 8 Vglut1-Cre and 8 WT mice ) mice subjected to the Barnes Maze (see methods section for Barnes Maze) task (Fig. 04-05). All groups repeated the task 3 times a day for 4 days, during which parameters for latency, speed, distance traveled and errors (investigating false escape holes) to complete the task were recorded and measured through the AnyMaze Software. See Methods for protocol differentiation. We found that all three groups, VGlut1-Cre and Gad2-Cre (adapted protocol) and WT (traditional protocol) presented progressive learning in the BM task. All animals presented lower latency, distance and fewer errors to complete the task throughout the days **(Fig. 5-A-C-E)**, however, differences between experimental groups were also significant. WT animals submitted to the traditional protocol, presented significantly lower values throughout all experimental days within errors, latency and distance traveled **(Fig. 5-A-C-E)**. To verify if these differences were due to abnormal learning rates, rather than differences in task difficulty, we analyzed the percentage change for each parameter among groups, and found that when change is applied from day 1 to 4, progressive learning is observer, however, differences among groups are not maintained **(Fig. 5-B-D-F)**.

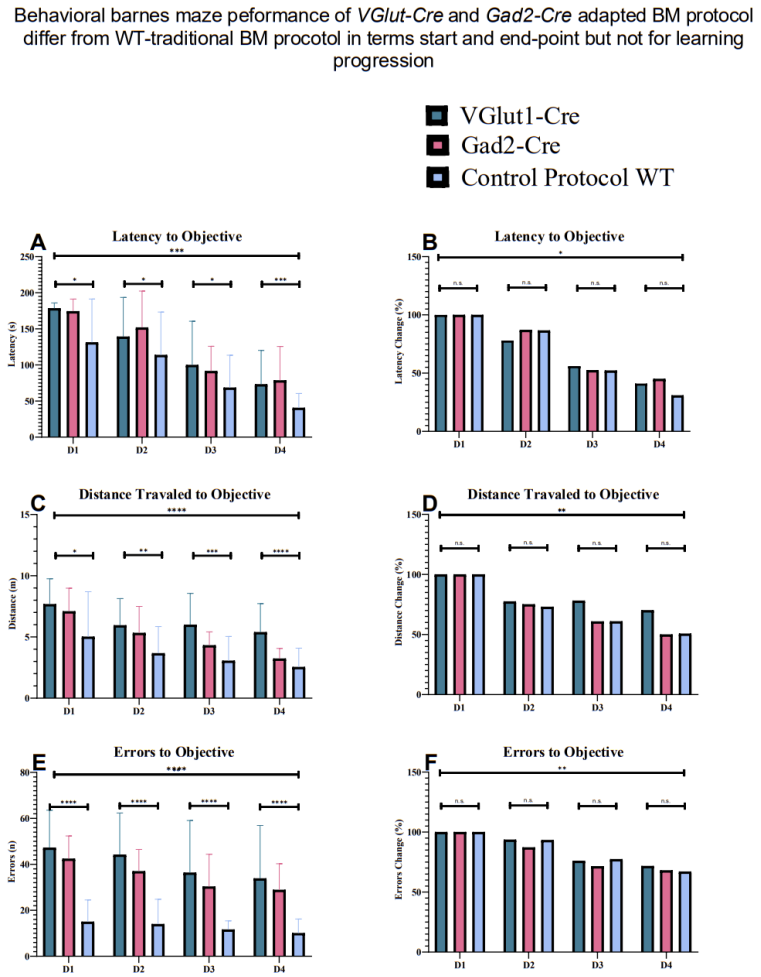


**Fig: 05 - Behavioral Barnes Maze performance of *VGlut1-Cre* and *Gad2-Cre* adapted BM protocol differ from WT-traditional BM protocol in terms of start and end-point performance, but not for learning progression.**
Graphs: At x-axis days 01 to day 04 of the Barne´s Maze behavioral task. At y-axis - **A** Latency (s) overall assessment $p \leq 0.0001$. **B:** Latency Change (%) overall assessment $p \leq 0.0001$. **C:** Distance traveled (m) overall assessment $p \leq 0.0051$. **D:** Distance Change (%) overall assessment $p \leq 0.024$. **E:** Errors (n) overall assessment $p \leq 0.052$. **F:** Error Change (%) overall assessment $p \leq 0.0001$
Seconds (s), meters (m), quantity (n), meters per second (m/s), days (D) average (Avg.), percentage (%), *$p \leq 0.05$, **$p \leq 0.01$, *** $\leq 0.001$, ****$p \leq 0.0001$. Overall assessment one-way ANOVA with daily differences Tukey's multiple comparisons test. Bars are standard deviation from mean value.

## 3.2 Both *VGlut1-Cre* and *Gad2-Cre* biosensor-injected mice present progressive performance throughout the Barnes Maze task for both total and primary results.

Once our protocol was validated, we moved forward to analyze the overall performance of *VGlut1-Cre* and *Gad2-Cre* bionsensor injected mice in the BM task **(Fig. 6-7).** To determine whether data collected from FIP during the Barnes Maze would be representative from a cognitive base task, we analyzed both total and primary performances for *VGlut1-Cre* and *Gad2-Cre* mice from day 1 to 4.

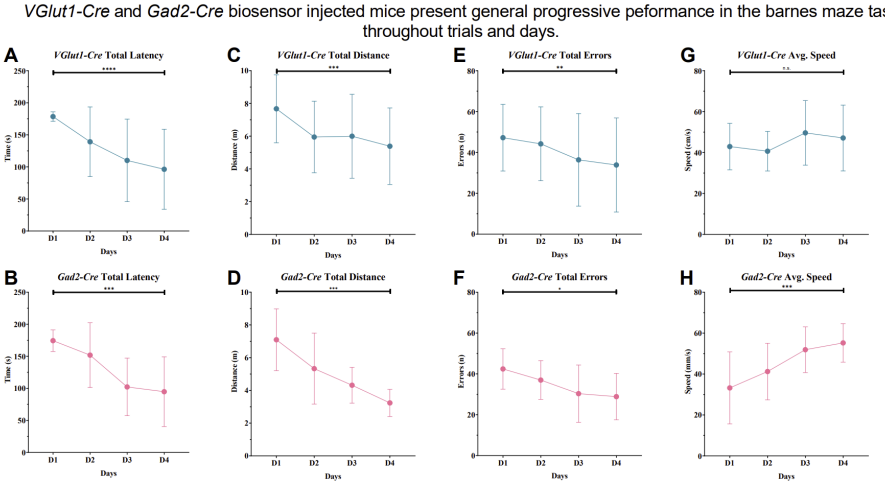


**Fig: 06 - *VGlut1-Cre* and *Gad2-Cre* biosensor-injected mice present general progressive performance in the Barnes Maze task throughout trials and days.**

Graphs: At x-axis days 01 to day 04 of the Barne´s Maze behavioral task. At y-axis - **A:** *VGlut1-Cre* Latency (s) overall assessment $p \leq 0.0001$. **B:** *Gad2-Cre* Latency (s) overall assessment $p \leq 0.001$. **C:** *VGlut1-Cre* Distance traveled (m) overall assessment $p \leq 0.0009$. **D:** *Gad2-Cre* Distance traveled (m) overall assessment $p \leq 0.0006$ **E:** *VGlut1-Cre* Errors (n) overall assessment $p \leq 0.008$. **F:** *Gad2-Cre* Errors (n) overall assessment $p \leq 0.019$ **G:** *VGlut1-Cre* Avg. Speed (cm/s) overall assessment $p \leq 0.04$ **H:** *Gad2-Cre* Avg. Speed (cm/s) overall assessment $p \leq 0.01$.
Seconds (s), meters (m), quantity (n), meters per second (m/s), days (D) Average (Avg.), *$p \leq 0.05$, **$p \leq 0.01$, *** $\leq 0.001$, ****$p \leq 0.0001$. Overall assessment one or two-way ANOVA with daily differences Tukey's multiple comparisons test.

**Fig: 07 - *VGlut1-Cre* and *Gad2-Cre* biosensor-injected mice present primary progressive performance in the Barnes Maze task throughout trials and days.**

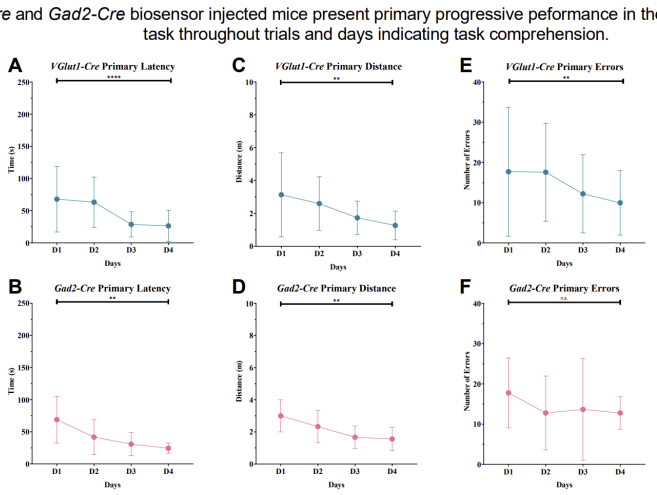


Graphs: At x-axis days 01 to day 04 of the Barne´s Maze behavioral task. Primary data. At y-axis - **A:** *VGlut1-Cre* Primary Latency (s) overall assessment $p \leq 0.0001$. **B:** *Gad2-Cre* Primary Latency (s) overall assessment $p \leq 0.023$. **C:** *VGlut1-Cre* Primary Distance traveled (m) overall assessment $p \leq 0.0010$. **D:** *Gad2-Cre* Primary Distance traveled (m) overall assessment $p \leq 0.0085$. **E:** *VGlut1-Cre* Primary Errors (n) overall assessment $p \leq 0.0014$ **F:** *Gad2-Cre* Primary Errors (n) overall assessment $p \leq 0.55$
Seconds (s), meters (m), quantity (n), meters per second (m/s), days (D) Average (Avg.), *$p \leq 0.05$, **$p \leq 0.01$, *** $\leq 0.001$, ****$p \leq 0.0001$. Overall assessment one or two-way ANOVA with daily differences Tukey's multiple comparisons test. Bars are standard deviation from mean value.

Total performance analysis shows that both *VGlut1-Cre* and *Gad2-Cre* groups presented significant lower latency **(Fig. 6-A-B)**, distance traveled **(Fig. 6-C-D)** and errors **(Fig. 6-E-F)** from day 1 to 4. Significant differences for average speed during the task was observed only in the *Gad2-Cre* group **(Fig. 6-G-H).** Consistently, primary data presented significant differences in all domains for both groups: latency **(Fig. 7-A-B)**, distance **(Fig. 7-C-D)** and errors **(Fig. 7-E-F)**. In addition to observing basic quantitative performance parameters, qualitative adopted strategy was observed for each mouse **(Fig. 8-C)**. Both Gad2-Cre and VGlut1-Cre mice

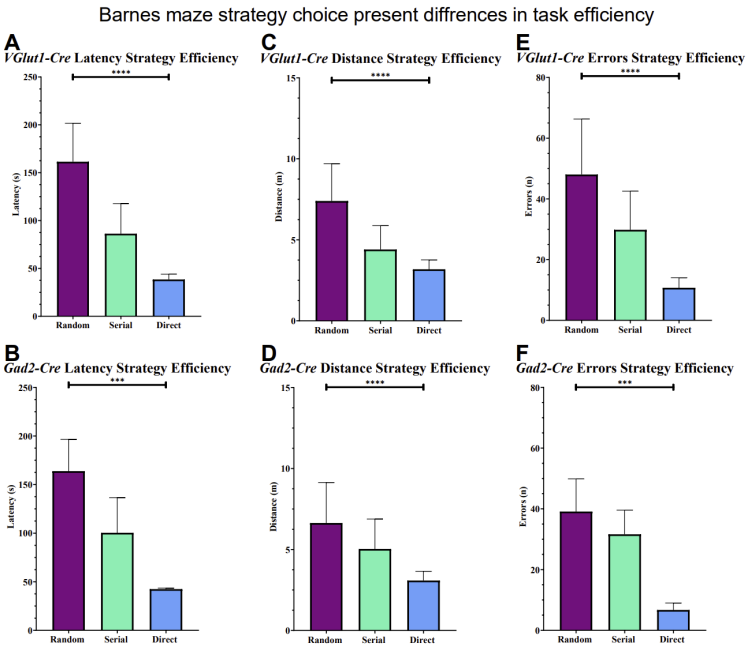

presented decreasing percentages of random strategies while presenting a progressive increase in serial and direct strategies throughout the days **(Fig. 8-A-B)**.

**Fig: 08 - *VGlut1-Cre* and *Gad2-Cre* biosensor-injected mice present adaptation to more efficient strategies throughout the Barnes Maze task.**
Graphs: At x-axis summed adopted from all trials. Adopted Strategy. At y-axis - **A:** *VGlut1-Cre* Adopted Strategy (%) overall assessment $p \leq 0.01$. **B:** *Gad2-Cre* Adopted Strategy (%) overall assessment $p \leq 0.0.009$. **C:** Strategy types, from right to left: Random, Serial And Direct strategies from one animal in trials in D1, D2 and D4. Percentage (%), days (D) Average (Avg.), *$p \leq 0.05$, **$p \leq 0.01$, *** $\leq 0.001$, ****$p \leq 0.0001$. Overall assessment one or two-way ANOVA with daily differences Tukey's multiple comparisons test. Bars

Furthermore, we cross-assessed latency, distance traveled and errors performance when each strategy was adopted **(Fig. 9)**. Performances for both groups were analyzed individually, in which we found that, animals who adopted the direct strategy presented the lowest latency **(Fig. 9-A-B)**, distance traveled **(Fig. 9-C-D)** and errors **(Fig. 9-E-F)** in contrast to animals that adopted random strategies, presenting the highest values for all 3 parameters, with the serial strategy at the middle.

**Fig: 09 - Barnes Maze strategy choice presents differences in task efficiency.**
Graphs: At x-axis summed adopted strategy from all trials. Adopted Strategy Efficiency. At y-axis - **A:** *VGlut1-Cre* Latency(s)/Strategy overall assessment $p \leq 0.0001$. **B:** *Gad2-Cre* Latency(s)/Strategy overall assessment $p \leq 0.0001$. **C:** *VGlut1-Cre* Distance(m)/Strategy overall assessment $p \leq 0.0001$. **D:** *Gad2-Cre* Distance(m)/Strategy overall assessment $p \leq 0.0001$. **E:** *VGlut1-Cre* Errors(n)/Strategy overall assessment $p \leq 0.0001$ **F:** *Gad2-Cre* Errors(n)/Strategy) overall assessment $p \leq 0.0001$
Seconds (s), meters (m), quantity (n), meters per second (m/s), days (D) Average (Avg.), *$p \leq 0.05$, **$p \leq 0.01$, *** $\leq 0.001$, ****$p \leq 0.0001$. Overall assessment one or two-way ANOVA with daily differences Tukey's multiple comparisons test. Bars are standard deviation from mean value.

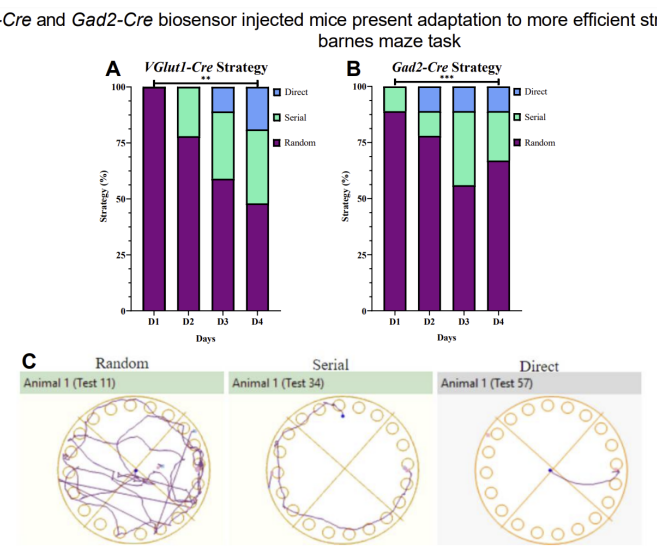


## 3.3 VGlut1-Cre and Gad2-Cre jGCaMP6f injected mice daily fiber photometry data

In sequence, we looked to analyze the activation patterns of *Gad2* and *VGlut1* positive neurons throughout the BM daily trials. Data presented for FIP represent either the average Z-Score variation of fluorescence (Z-ΔF/F) or the number of Z-Score significant events (Z-ΔF/F Event Count). Peak activity was isolated within each behavior context: activity when

investigating escape chamber, error holes, non-paired (no context) and total (chmaber+errors+non-paired). *VGlut1-Cre* biosensor injected animals (glutamatergic activity), presented significant increasing peak activity from day 1 to 4 for escape chamber investigation , non-paired contexts and total activity **(Fig. 10-A-E-G)**. No differences were detected for error hole context **(Fig. 10-C)**. *Gad2-cre* biosensor injected animals (gabaergic activity) showed a significant decrease in peak activity from day 1 to 4 for error hole investigation **(Fig. 10-B)**, while no other significant change was detected for other contexts **(Fig. 10-D-F-H)**.

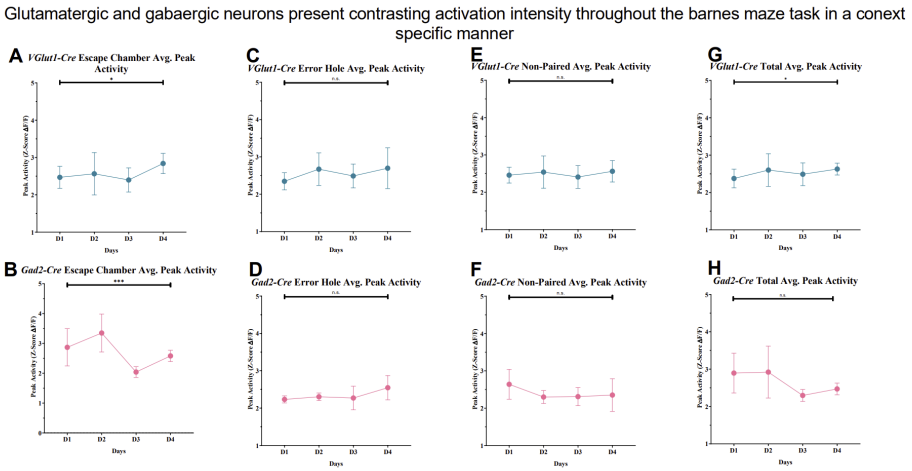


**Fig: 10 - Glutamatergic and gabaergic neurons present contrasting activation intensity throughout the Barnes Maze task in a context specific manner.**
Graphs: At x-axis days 01 to day 04 of the Barne´s Maze behavioral task. At y-axis - **A:** *VGlut1-Cre* peak activity (Z-Score Δf/f) in escape chamber overall assessment $p \leq 0.031$ **B:** *Gad2-Cre* peak activity (Z-Score Δf/f) in escape chamber overall assessment $p \leq 0.0004$ **C:** *VGlut1-Cre* peak activity (Z-Score Δf/f) in error holes overall assessment $p \leq 0.21$ **D:** *Gad2-Cre* peak activity (Z-Score Δf/f) in error holes overall assessment $p \leq 0.45$. **E:** *VGlut1-Cre* peak activity (Z-Score Δf/f) for non-paired overall assessment $p \leq 0.44$. **F:** *Gad2-Cre* peak activity (Z-Score Δf/f) for non-paired overall assessment $p \leq 0.33$ **G:** *VGlut1-Cre* peak activity (Z-Score Δf/f) total overall assessment $p \leq 0.046$ **H:** *Gad2-Cre* peak activity (Z-Score Δf/f) total overall assessment $p \leq 0.062$
Z-Score Δf/f (Variation of fluorescence over fluorescence in deviations), Seconds (s), meters (m), quantity (n), meters per second (m/s), days (D) Average (Avg.), *p ≤ 0.05, **p ≤ 0.01, *** ≤ 0.001, ****p ≤ 0.0001. Overall assessment one or two-way ANOVA with daily differences Tukey's multiple comparisons test.

Furthermore, the number of significant events is also a trace that could indicate changes in firing patterns within each neuronal type. To do so, we normalized the total number of events by the total task latency within each context. This was done since each trial presented contrasting total and primary latency from day-to-day and trial-to-trial, meaning that an increase or decrease in number of events could be modulated

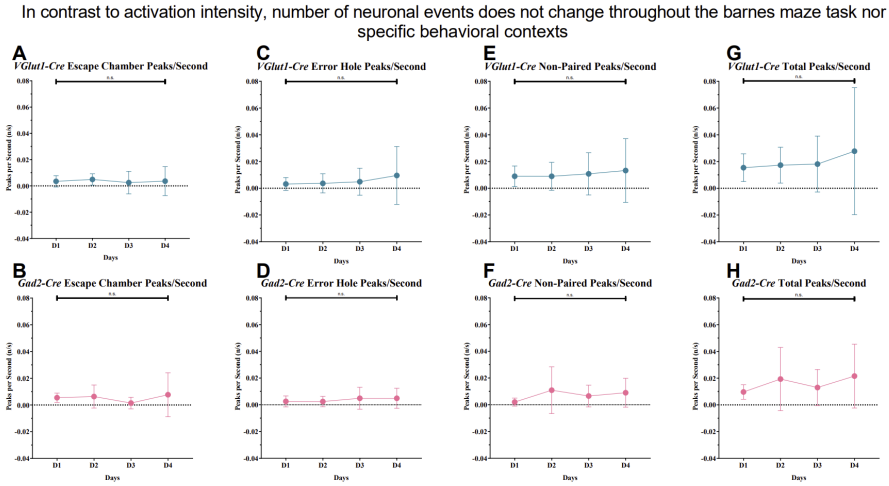

by exposure time to the task. However, neither *VGlut1* and *Gad2* positive neurons presented significant differences in the number of neuronal events/second throughout the BM task **(Fig. 11-A-B-C-D-E-F-G-H).**

**Fig: 11 - In contrast to activation intensity, the number of neuronal events does not change throughout the Barnes Maze task nor in specific behavioral contexts.**

Graphs: At x-axis days 01 to day 04 of the Barne´s Maze behavioral task. At y-axis - **A:** *VGlut1-Cre* number of peaks/second in escape chamber overall assessment $p \leq 0.63$ **B:** *Gad2-Cre* number of peaks/second in escape chamber overall assessment $p \leq 0.52$ **C:** *VGlut1-Cre* number of peaks/second in error holes overall assessment $p \leq 0.26$ **D:** *Gad2-Cre* number of peaks/second in error holes overall assessment $p \leq 0.66$. **E:** *VGlut1-Cre* number of peaks/second for non-paired overall assessment $p \leq 0.63$. **F:** *Gad2-Cre* number of peaks/second for non-paired overall assessment $p \leq 0.39$ **G:** *VGlut1-Cre* number of peaks/second total overall assessment $p \leq 0.30$ **H:** *Gad2-Cre* number of peaks/second total overall assessment $p \leq 0.48$

Z-Score Δf/f (Variation of fluorescence over fluorescence in deviations), Seconds (s), meters (m), quantity (n), meters per second (m/s), days (D) Average (Avg.), *p ≤ 0.05, **p ≤ 0.01, *** ≤ 0.001, ****p ≤ 0.0001. Overall assessment one or two-way ANOVA with daily differences Tukey's multiple comparisons test.

Furthermore, both peak intensity and number of events were segregated by trial, and then allocated into categories of adopted strategy. Meaning that we compared the activation patterns for each trial when animals adopted one of three present strategies. In addition, neuronal patterns were seeked within each behavioral context, chamber and error hole investigation, non-paired and total. Hence resulting in activation patterns, happening within each context, segregated by adopted strategy. We found that both *VGlut-Cre* and *Gad2-Cre* presented none to significantly lower activation patterns within investigating the escape chamber for animals that adopted the direct strategy in contrast to random and serial **(Fig. 12-A-B).** This profile was maintained for error hole investigation and total activation patterns per strategy for *VGlut1-Cre* mice **(Fig. 12-C-G)** but not for non-paired activity **(Fig. 12-E).** No other significant change was seen within *Gad2-Cre* activation patterns **(Fig. 12-D-F-H)**.

Curiously, stronger results were detected when the same analysis was done, but in regards to the number of events instead of intensity **(Fig. 13)**. *VGlut1-Cre* mice presented a significantly lower number of events in chamber investigation for the direct strategy in comparison to random and serial **(Fig. 13-A)**, in contrast, number of events for escape

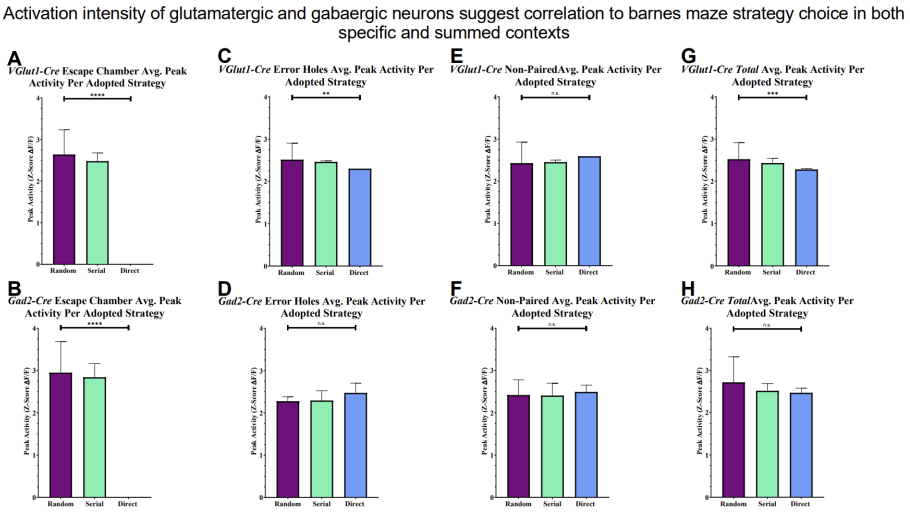

hole, non-paired and total contexts within the direct strategy were significantly higher compared to random and serial **(Fig. 13-C-E-G)**.

**Fig: 12 - Activation intensity of glutamatergic and gabaergic neurons suggest correlation to Barnes Maze strategy choice in both specific and summed contexts.** Graphs: Graphs: At x-axis summed adopted strategy from all trials. At y-axis - **A:** *VGlut1-Cr*e peak activity (Z-Score **Δ**f/f) in escape chamber overall assessment $p \leq 0.0001$ **B:** *Gad2-Cre* peak activity (Z-Score **Δ**f/f) in escape chamber overall assessment $p \leq 0.0001$ **C:** *VGlut1-Cr*e peak activity (Z-Score **Δ**f/f) in error holes overall assessment $p \leq 0.0063$ **D:** *Gad2-Cre* peak activity (Z-Score **Δ**f/f) in error holes overall assessment $p \leq 0.27$. **E:** *VGlut1-Cre* peak activity (Z-Score **Δ**f/f) for non-paired overall assessment $p \leq 0.42$. **F:** *Gad2-Cre* peak activity (Z-Score **Δ**f/f) for non-paired overall assessment $p \leq 0.40$ **G:** *VGlut1-Cre* peak activity (Z-Score **Δ**f/f) total overall assessment $p \leq 0.0001$ **H:** *Gad2-Cre* peak activity (Z-Score **Δ**f/f) total overall assessment $p \leq 0.12$
Z-Score **Δ**f/f (Variation of fluorescence over fluorescence in deviations), Seconds (s), meters (m), quantity (n), meters per second (m/s), days (D) Average (Avg.), *$p \leq 0.05$, **$p \leq 0.01$, *** $\leq 0.001$, ****$p \leq 0.0001$. Overall assessment one or two-way ANOVA with daily differences Tukey's multiple comparisons test.

*Gad2-Cre* mice followed similar significant results for number of events for escape hole, non-paired and total contexts within the direct strategy **(Fig. 13-D-F-H)**, however no change was observed for number of events in chamber investigation for the direct strategy **(Fig. 13-B)**.

**Fig: 13 - Number of neuronal events for both glutamatergic and gabaergic suggest correlation to Barnes Maze strategy choice in both specific and summed contexts.**
Graphs: Graphs: At x-axis summed adopted strategy from all trials. **A:** *VGlut1-Cr*e number of peaks/second in escape chamber overall assessment $p \leq 0.0001$ **B:** *Gad2-Cre* number of peaks/second in escape chamber overall assessment $p \leq 0.13$ **C:** *VGlut1-Cr*e number of peaks/second in error holes overall assessment $p \leq 0.0001$ **D:** *Gad2-Cre* number of peaks/second in error holes overall assessment $p \leq 0.021$ **E:** *VGlut1-Cre* number of peaks/second for non-paired overall assessment $p \leq 0.0001$ **F:** *Gad2-Cre* number of peaks/second for non-paired overall assessment $p \leq 0.0001$ **G:** *VGlut1-Cre* number of peaks/second total overall assessment $p \leq 0.0001$ **H:** *Gad2-Cre* number of peaks/second total overall assessment $p \leq 0.001$

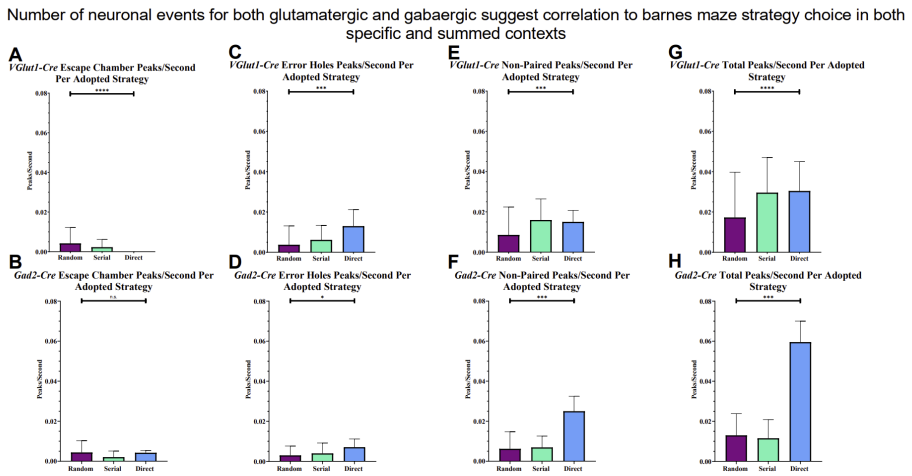


Z-Score **Δ**f/f (Variation of fluorescence over fluorescence in deviations), Seconds (s), meters (m), quantity (n), meters per second (m/s), days (D) Average (Avg.), *$p \leq 0.05$, **$p \leq 0.01$, *** $\leq 0.001$, ****$p \leq 0.0001$. Overall assessment one or two-way ANOVA with daily differences Tukey's multiple comparisons test.

# 4.0 DISCUSSION

Understanding the link between specific brain regions and their resident neuron population is what allows us to further recognize, contextualize, and maybe even prevent or treat brain based diseases. For many years brain regions were delimited in large portions and only a handful of contextualized behaviors could be associated to them (GENON S., 2018). Here, we presented an initial attempt to understand the activation patterns of both glutamatergic and gabaergic neurons within the mPFC of mice while performing learning, memory and decision making based tasks.

The Barnes Maze task is considered a complex task with multiple parameters to be observed. Since its initial appearance in studies by Barnes, C. A. (1979) other variations of this test have appeared. However, due to its complex protocol and structure, including height and escape chamber, no other studies have tried to investigate activation patterns of mice in online BM task performance. Overall data for *VGlut1-Cre* and *Gad2-Cre* mice presented contrasting results to literature in all domains (GAWEL. K., 2019), such as diminishing in latency, errors and distance traveled throughout task days **(Fig. 05-A-C-E)**. This result was expected due to locomotion difficulties presented once attached to optical fibers of the FIP system. However, when change (%) was analyzed from day one to day 4 for the same data, both *VGlut1-Cre* and *Gad2-Cre* animals that were attached to FIP system under modified BM, presented no differences in comparison to WT-control (traditional protocol with no FIP) **(Fig. 05-B-D-F)**. These results consist that although the starting point and end point for latency, distance and errors in each group is different **(Fig. 05-A-C-E)**, their learning capabilities and rates are equal **(Fig. 05-B-D-F),** and that these differences, however may they be from a more difficult task due to adaptations, they do not mischaracterize the BM task.

Furthermore, our objective here was not to compare neither cognitive performances nor neuronal activity between *VGlut1-Cre* and *Gad2-Cre* mice, but to determine whether mPFC neurons for these subgroups present specific and adaptable neuronal patterns in mice subjected to cognitive tasks. Unfortunately, comparing neuronal activity provenient from two different groups of neurons is extremely complex, considering contrasting quantities of population density within the mPFC, which by itself results in significant differences in activity. Normalization of this data could be done by Mini-Scope, where FIP results are accompanied by imaging allowing us to determine the quantity of neurons responsive in each

situation and serving as a normalizing value. However, the technique in question is very recent and complex, and has yet to become accessible due to pricing and distribution. Hence, in the following discussion, data for each group will be compared within itself.

In general, both experimental groups presented significant progressive learning during the BM task in one or more parameters. From each trial and day of task mice naturally present improvement in performance which in terms represents a learning remark. Overall, *VGlut1-Cre* and *Gad2-Cre* biosensor injected mice showed significant learning progression in both total and primary results, such as diminishing latency, distance and errors **(Fig 06-A-B-C-D-E-F and 07-A-B-C-D-E-F)**. Primary and total data are shown separately. The use of primary data as seen here is mostly presented to demonstrate whether animals have learned the task. Throughout the task it is common for animals to lose interest in achieving the objective (entering the escape chamber and returning to its housing cage). This happens due to the constant repetition and lack of change in the process, especially if no reward is paired to task execution (sugar based food) or the evasion of an aversive stimulus (intense lighting, wind, cold and more…) is present. Hence, primary data is shown to demonstrate that animals are capable of accurately locating the escape chamber with increasing performance throughout trials, in spite of not entering the chamber itself and choosing to continue exploring the apparatus. Here no reward nor aversive stimulus was used to motivate task execution, since by doing so these have the potential of strongly modulating mPFC neurons and by then hiding our targeted context, which is understanding the activation patterns of mPFC neurons during learning, memory and decision making.

In addition to progressive learning, both groups adopted different strategies (serial **(Fig 08-C-Middle)** and direct **(Fig 08-C-Right)**) throughout the task **(Fig 08-A-B-C).** Serial strategies were seen to be the most efficient. Mice that adopted this strategy presented the lowest number of errors **(Fig 09-A-B)**, latency **(Fig 09-C-D)** and distance traveled **(Fig 09-E-F)**. As opposed to the random **(Fig 08-C-Left)** strategy, which showed the highest numbers for errors, latency and distance traveled. The serial strategy was seen to be put in between them.

Strategy choice easily reflexes all three domains within this task. Choosing more efficient strategies based on experience due to reexposure is a basic trait of decision making (HULLERMEIER., 2001), of which a decision maker's experience is based on past events (good or not). Whether these adaptations were made consciously or instinctively extrapolates the scope of this study, but should be discussed and investigated in future projects.

With the behavior protocol in line, and data for both groups presenting progressive learning with adaptable efficient strategies, we moved forward to analyze whether *VGlut1* positive or *Gad2* positive neuronal activation patterns would change when crossed with behavioral data. Therefore, we began investigating patterns for each group from day 1 to 4.

Peak activity/intensity was detected for both glutamatergic and gabaergic neurons in distinct mice. Data was segregated into activity for when animals explored the escape chamber, error holes, non-paired and the total sum of all three ques. Interestingly, increasing peak activity (D1 to D4) provenient from glutamatergic neurons was directly accompanied by decreasing peaks from gabaergic neurons when exclusively exploring the escape chamber **(Fig 10-A-B)**. This was not observed in any other que **(Fig 10-C-D-E-F-G-H)**. Gabaergic neurons are largely known as inhibitory neurons, and possess large control over the function of cortical networks, regulating the development of the brain by moderating the proliferation and connectivity of neurons (HUANG., 2019). In contrast glutamatergic neurons are commonly known as primary excitatory stations within the nervous system (REINER., 2018). Both present a vast body of functions and correlation to behavioral contexts. Previous research has highlighted the role of glutamate and gamma-aminobutyric acid (GABA) in learning and plasticity and that GABA itself possesses strong inhibitory regulation over glutamatergic neurons (STANLEY., 2017). Hence, the dynamic between increase and decrease of glutamatergic and gabaergic signals, respectively, are consistent with literature. Furthermore, this dynamic seems to play an important role in the learning achievement process of the BM task, since when errors or no context was observed this dynamic was not maintained. An increase in glutamatergic activity could also translate to a reward based activation (HORST., 2013), however, since this pattern was made evident, not from the beginning of the task but throughout the days in which accompanies learning, it is suggestive that this specific pattern is directly paired to a learning process. A second pattern that could aggregate to this dynamic is whether the increase in activity was due to higher number of events within our targeted neurons rather than more intensive activations and inhibitions. The mPFC is a high intensity brain region with constant brain activity, hence backround activation could have been a factor for both hiding and misleading task associated activation intensity (EUSTON D.R., 2012), therefore, we moved to analyze whether the number of significant fluorescent events (based on Z-Score deviation 2+) changed. Yet, the number of peak events/second within each context presented no significant changes **(Fig 11-C-D-E-F-G-H)**.

In spite of the main differences being seen in fluorescente provenient from glutamatergic neurons, Gad2 alterations under cognitive behavior may not be dismissed. In

addition to the necessity of a higher number of samples, the mPFC presents a predominance in glutamatergic (pyramidal cells) over gabaergic neurons (ALLEN BRAIN MAP - REFERENCE ATLAS). Therefore, alteration in Gad2 neurons may be more discrete and yet to be detected. Overall, data presented for VGlut1 groups are novel, thus also requiring further validation. However, there have been robust results in literature that complement and may even corroborate our findings. In spite of no other context present significant changes in neither activity intensity nor number of activations, we sought to investigate the means through which the escape chamber is located during this task. Curiously, we found that when activation events/intensity was separated into whether they happened during random ,serial or direct strategies significant changes could be observed . We found that both glutamatergic and gabaergic neurons presented low to null activity for when the most efficient strategy (direct) was adopted compared to random and serial while investigating the escape chamber **(Fig 12-A-B)**. Serial results also presented lower levels when compared to the least efficient strategy (random) **(Fig 12-A-B)**. Additionally, proportionally inverted results were found for activation intensity in strategies for when the error hole is investigated **(Fig 12-C-D)**, compared to what was seen in for activation intensity in the escape chamber **(Fig 10-A-B)**. The number of events within each context and strategy were also significantly different **(Fig 13)**. With the exception for number of activation events/second of gabaergic neurons separated by adopted strategy **(Fig 13-B)**, all other context, presented increasing number of peak events in order of least efficient strategy (less activation events/second) to most efficient strategy (more activation events/second) **(Fig 13-A-C-D-E-F-G-H)**. The correlation of mPFC neurons and strategy lack in the body of literature, however we have found studies that concluded the mFPC neurons are able to predict shifts in adopted strategy (SCHUCK., 2015). However these studies analyzed general neuronal activation patterns, with no distinction in neuronal type nor circuit connectivity. With the residing data in hands, we sorted through literature to better understand the relationship of our data and existing studies.

The mPFC is connected to multiple areas through neuronal inputs and outputs (BITTAR T.P., 2021) and plays an important role in executive function maintenance such as working memory, decision making, attentional selection and behavioral inhibition (Granon, Vidal, Thinus-Blanc, Changeux, & Poucet, 1994; Kesner & Churchwell, 2011; Rich & Shapiro, 2007). Additionally, hippocampal CA1 projections to the mPFC have been shown to play an important role in the retrieval of recent and remote memories of mice in the inhibitory avoidance test (GONZALES C., 2013). However, such modulation is shown to be true exclusively during episodes of clear learning of relevant actions (SINGH A., 2019). A study

conducted in primates, with the intention to further elucidate the responsiveness of PFC neurons to cognitive based tasks pre and post training revealed significant cortical plasticity mediated by cognitive tasks (XUE-LIAN Q., 2012). Another consistent signature of learning, among researchers, is that the reduction of neuronal activity, due to plasticity, during tasks is understood as an important stamp of expertise (BILALIC, M., 2010). Contrastingly, changes presented in raw activation intensity for chamber investigation do not reason with literature findings **(Fig 10-A-B)**, although this result could possibly be of some sort of reward based activation, since increasing neuronal activation within task based rewards have been known to present similar data (HORST., 2013). Hence, we theorize that changes shown in the diminishing activation intensity for more efficient strategies during escape chamber and error hole investigation may be provenient of expertise acquisition in the BM task **(Fig 12-13)**, meaning that the more efficient mice presented to be during the task, less activation was necessary to conclude the task.

# 5. CONCLUSION

In conclusion, the comprehension of which specific populations of both glutamatergic and gabaergic neurons within the mPFC play some sort of roll in cognitive task through specific activation patterns, offers not only the understanding over which cognition may be formed and associated circuits, but also potential targets and protocols to tackle specific cognitive impaired based diseases. Using such activation patterns through neurostimulation (optogenetics, transcranial magnetic stimulation, transcranial electric stimulation, ultrasound stimulation and more ) focalized over these specific populations could proportionate potentiation and rescue of faulty cognitive systems such as seen in dementia. However, there is yet much to be elucidated before these results and innovations can be extrapolated to human health. Hence, we offer our future perspectives, focusing on investigating the specific circuitry responsible for such results, as well as neuronal calcium imaging and forced modulation through optogenetics, which in part we believe would bring significant information corroborating our data above.

# 6. REFERENCES


1. Bassett, D. S., Yang, M., Wymbs, N. F., & Grafton, S. T. (2015). Learning-induced autonomy of sensorimotor systems. *Nature Neuroscience*, *18*(5), 744–751. https://doi.org/10.1038/nn.3993.

2. Bittar, T. P., & Labonté, B. (2021). Functional Contribution of the Medial Prefrontal Circuitry in Major Depressive Disorder and Stress-Induced Depressive-Like Behaviors. In *Frontiers in Behavioral Neuroscience* (Vol. 15). Frontiers Media S.A. https://doi.org/10.3389/fnbeh.2021.699592.

3. Charan, J., & Kantharia, N. (2013). How to calculate sample size in animal studies? In *Journal of Pharmacology and Pharmacotherapeutics* (Vol. 4, Issue 4, pp. 303–306). https://doi.org/10.4103/0976-500X.119726.

4. Genon, S., Reid, A., Langner, R., Amunts, K., & Eickhoff, S. B. (2018). How to Characterize the Function of a Brain Region. In *Trends in Cognitive Sciences* (Vol. 22, Issue 4, pp. 350–364). Elsevier Ltd. https://doi.org/10.1016/j.tics.2018.01.010.

5. Gonzalez, C., Kramar, C., Garagoli, F., Rossato, J. I., Weisstaub, N., Cammarota, M., & Medina, J. H. (2013). Medial prefrontal cortex is a crucial node of a rapid learning system that retrieves recent and remote memories. *Neurobiology of Learning and Memory*, *103*, 19–25. https://doi.org/10.1016/j.nlm.2013.04.006.

6. Gunaydin, L. A., Grosenick, L., Finkelstein, J. C., Kauvar, I. v., Fenno, L. E., Adhikari, A., Lammel, S., Mirzabekov, J. J., Airan, R. D., Zalocusky, K. A., Tye, K. M., Anikeeva, P., Malenka, R. C., & Deisseroth, K. (2014). Natural neural projection dynamics underlying social behavior. *Cell*, *157*(7), 1535–1551. https://doi.org/10.1016/j.cell.2014.05.017.

7. Koop, L. K., Prasanna, ;, & Affiliations, T. (2021). *Neuroanatomy, Sensory Nerves*. https://www.ncbi.nlm.nih.gov/books/NBK539846/?report≤printable.

8. Lee, I., & Lee, C. H. (2013). Contextual behavior and neural circuits. In *Frontiers in Neural Circuits* (Issue APR 2013). https://doi.org/10.3389/fncir.2013.00084.

9. Manivannan, M., & Suresh, P. K. (2012). On the somatosensation of vision. *Annals of Neurosciences*, *19*(1), 31–39. https://doi.org/10.5214/ans.0972.7531.180409.

10. Martianova, E., Aronson, S., & Proulx, C. D. (2019). Multi-fiber photometry to record neural activity in freely-moving animals. Journal of Visualized Experiments, 2019(152). https://doi.org/10.3791/60278 .

11. Mcdougall, G. J., & Bolton, F. P. (1995). *A Critical Review of Research on Cognitive Function/Impairment in Older Adults*.

12. Nozawa, T., Taki, Y., Kanno, A., Akimoto, Y., Ihara, M., Yokoyama, R., Kotozaki, Y., Nouchi, R., Sekiguchi, A., Takeuchi, H., Miyauchi, C. M., Ogawa, T., Goto, T., Sunda, T., Shimizu, T., Tozuka, E., Hirose, S., Nanbu, T., & Kawashima, R. (2015). Effects of Different

Types of Cognitive Training on Cognitive Function, Brain Structure, and Driving Safety in Senior Daily Drivers: A Pilot Study. *Behavioural Neurology*, *2015*. https://doi.org/10.1155/2015/525901.

13. Pitts MW. Barnes Maze Procedure for Spatial Learning and Memory in Mice. Bio Protoc. 2018 Mar 5;8(5):e2744. doi: 10.21769/bioprotoc.2744. PMID: 29651452; PMCID: PMC5891830.

14. Pulvermüller, F., Garagnani, M., & Wennekers, T. (2014). Thinking in circuits: toward neurobiological explanation in cognitive neuroscience. *Biological Cybernetics*, *108*(5), 573–593. https://doi.org/10.1007/s00422-014-0603-9.

15. Qi, X. L., Meyer, T., Stanford, T. R., & Constantinidis, C. (2011). Changes in prefrontal neuronal activity after learning to perform a spatial working memory task. *Cerebral Cortex*, *21*(12), 2722–2732. https://doi.org/10.1093/cercor/bhr058.

16. Qi, X. L., & Constantinidis, C. (2013). Neural changes after training to perform cognitive tasks. In *Behavioural Brain Research* (Vol. 241, Issue 1, pp. 235–243). https://doi.org/10.1016/j.bbr.2012.12.017.

17. Singh, A., Peyrache, A., & Humphries, M. D. (2019). Medial prefrontal cortex population activity is plastic irrespective of learning. *Journal of Neuroscience*, *39*(18), 3470–3483. https://doi.org/10.1523/JNEUROSCI.1370-17.2019.

18. Sohmer, H., & Freeman, S. (2000). *BASIC AND CLINICAL PHYSIOLOGY OF THE INNER EAR RECEPTORS AND THEIR NEURAL PATHWAYS IN THE BRAIN* (Vol. 11, Issue 4).

19. Surís, A., Holliday, R., & North, C. S. (2016). The evolution of the classification of psychiatric disorders. *Behavioral Sciences*, *6*(1). https://doi.org/10.3390/bs6010005.